Spectral Theory of Turbulent Heat Transfer in the Presence of a Rough Wall

Peeters, Jurriaan W.R.

Important note
To cite this publication, please use the final published version (if applicable).
Please check the document version above.

Spectral Theory of Turbulent Heat Transfer in the Presence of a Rough Wall

Jurriaan W. R. Peeters◉

Process and Energy, Mechanical Engineering, Delft University of Technology Leeghwaterstraat 39, 2628CB, Delft Netherlands

Using the phenomenological theory of turbulence, a direct link between the Stanton number—a dimensionless number that represents the ratio of transferred heat to the thermal capacity of the fluid—and the scalar spectrum is established for both smooth wall and rough wall conditions. The effect of different scales of motion on heat transfer is demonstrated by investigating relevant limits of the scalar spectrum. It is shown that two important observations in literature—the lack of increase in heat transfer beyond a certain roughness size and the nonclassical Prandtl number scaling—are reproduced if only the viscous inertial and diffusive range of the scalar spectrum is accounted for.

Most fluid flows in both nature and industry are turbulent flows. A turbulent flow is characterized by the formation of vortices, which break up into smaller and smaller vortices [1,2]. This phenomenon is well described by phenomenological theory as well as power law spectra. Even so, turbulence is a phenomenon from classical physics that is not yet fully understood to this day. This is especially the case for turbulent flows in the presence of a rough wall [3,4]. A wall is hydrodynamically rough when its topological features are large enough to affect the smallest eddies close to the wall. In phenomenological theory [5,6], the Kolmogorov length scale η is said to represent the size of the smallest eddy. Then, if the rough wall can be characterized by a length scale k, the turbulent flow can be said to be affected when $k > \eta$.

The most well-known description of the effect of wall roughness is the Moody diagram, which relates the friction factor (a measure of the shear stress τ_w exerted on the wall) to the bulk Reynolds number $\mathrm{Re} = U_b D/\nu$ (where U_b is the time averaged bulk velocity, D the hydraulic diameter, and ν the kinematic viscosity) and the wall roughness length scale k for turbulent pipe flows. However, a more convenient method to describe the effect of roughness on drag exists. Prandtl [7] showed that for flows past a smooth wall, the time averaged velocity can be described by the relation $U_s^+ = \kappa^{-1} \ln y^+ + A$, where the subscript s denotes smooth wall conditions, $U_s^+ = U_s/u_\tau$ ($u_\tau \equiv \sqrt{\tau_w/\rho}$ is the friction velocity, τ_w is the wall shear stress, and ρ is the fluid density), $y^+ \equiv y u_\tau/\nu$, $\kappa \approx 0.4$ is the von Karman constant, and $A \approx 5.1$. Similarly, for a rough wall, $U_r^+ = \kappa^{-1} \ln(y/k) - B(k^+)$ (where $k^+ \equiv u_\tau k/\nu$). Clauser [8] and Hama [9] exploited these log laws to define a roughness function $\Delta U^+ = U_s^+ - U_r^+ = \kappa^{-1} \ln(k^+) + A - B(k^+)$, which depends on k^+ only and where U_s^+ and U_r^+ are evaluated at matched y^+ and frictional Reynolds number $\mathrm{Re}_\tau \equiv u_\tau D/(2\nu)$. $\Delta U^+ > 0$ and $\Delta U^+ < 0$ correspond to

an increase and decrease in drag, respectively. Recent research shows that different surfaces appear to have a distinct roughness function, but also have an asymptote for large k^+ where B is no longer a function of k^+. Furthermore, ΔU^+ is directly related to the shear stress according to the relation $\Delta U^+ = \sqrt{2/C_{f,s}} - \sqrt{2/C_{f,r}}$, where the friction skin coefficients ($C_f \equiv 2\tau_w/\rho U_b^2$) are evaluated at matched Re_τ [10]. Thus, the effect of roughness on drag in a duct is completely described by the combination of Re and k/D or by Re_τ and k^+.

It is known that drag and heat transfer are affected differently by roughness as there is no pressure-drag analog for the latter [11–14]. Moreover, heat transfer is largely determined by the magnitude of the Prandtl number $\mathrm{Pr} = \nu/\alpha$ (where α is the thermal diffusivity). For ducts with roughness characteristics that are similar to sand grains, Dipprey and Sabersky [11] found that the Stanton number, $\mathrm{St} \equiv q/(\rho U_b c_p \Delta T)$, scales with $\mathrm{Pr}^{-0.44}$ when the roughness was relatively large; this scaling deviates significantly from the scaling in smooth wall conditions, i.e., $\mathrm{St} \sim \mathrm{Pr}^{-2/3}$. Here, q, c_p and ΔT refer to the wall heat flux, specific heat capacity and the difference between the wall- and bulk temperature, respectively.

The mean temperature profile in a heated duct can also be described by a log-law in smooth wall conditions and rough wall conditions [15]. MacDonald *et al.* [16] showed that a scalar roughness function $\Delta \Theta^+(k^+)$ which denotes the downward shift of the mean temperature profile at matched y^+ can be formulated. Like ΔU^+, $\Delta \Theta^+ > 0$ means an increase in heat transfer. Unlike ΔU^+, $\Delta \Theta^+$ approaches a constant value for large values of k^+. A similar trend was also found by Peeters and Sandham [17]. This means that there is a critical value k^+ beyond which heat transfer cannot be increased by enlarging the wall roughness. Furthermore, a relation between the Stanton number and the wall roughness function exists [16]:

$$\Delta\Theta^+ = \sqrt{\frac{C_{f,s}}{2}}\left(\frac{1}{\mathrm{St_s}} - \frac{\mathrm{Pr}_t}{\kappa^2}\right) - \sqrt{\frac{C_{f,r}}{2}}\left(\frac{\mathrm{Pr}_t}{\mathrm{St_r}} - \frac{1}{\kappa^2}\right), \quad (1)$$

where Pr_t is the turbulent Prandtl number, which represents the ratio of the turbulent mixing of momentum to that of heat. Equation (1) is valid when the Stanton numbers and skin friction coefficients are evaluated at matched Re_τ.

In this work, a relationship between the Stanton number and the power spectrum of thermal fluctuations is used to explain the trends of the scalar wall roughness function as well as the deviatory Prandtl number scaling. This relationship was previously derived by the author [18] through the extension of the work of Gioia and Chakraborty [19], who consider a rough surface whose elements are spaced apart by a distance equal to their height. Such a surface resembles the sand-grain surface that was used by Nikuradse [20] (consequently, the symbol k_s will be used instead of k hereafter). Using physical arguments, Gioia and Chakraborty [19] show that $\tau \sim \rho U_b u_s$. Here, u_s is the velocity of an eddy of size s, which is related to the spectrum of turbulent kinetic energy at a length scale σ as $u_s^2 = \int_0^s E(\sigma)\sigma^{-2}d\sigma$. Noting that the largest eddy that fits between two roughness elements has a dominant contribution to τ, a relation for C_f is ultimately derived:

$$C_f = K \int_0^{s/R} x^{-1/3} c_d\left(\frac{b'\mathrm{Re}^{-3/4}}{x}\right) c_e(x)dx, \quad (2)$$

where $K = 0.03$, $x = \sigma/R$, $s/R \equiv (2k_s/D) + ab'\mathrm{Re}^{-3/4}$, with $a = 3$ and $b' = 11.4 \times (1/2)^{-3/4}$. The functions $c_e(x) = [1 + \gamma x^2]^{-17/6}$ (with $\gamma = 6.783$) and $c_d(x) = \exp(-\beta_u z)$ (with $\beta_u = 2.1$) describe the energetic- and diffusive range of the spectrum, respectively [18,19].

The thermal analog of Eq. (2) is found by considering the eddy of size s and velocity υ shown in Fig. 1. The eddy transports relatively hot fluid ($t_s > 0$) away from the wall and relatively cold fluid ($t_s < 0$) toward it, creating two thermal structures of size s_ϕ. Both structures contribute positively to the net heat transfer rate across the plane W. Consequently, the net heat flux across W scales as $q \sim \rho c_p \upsilon t_s$.

The magnitude of the temperature of s_ϕ relative to T_b is related to the scalar spectrum E_ϕ as

$$t_s^2 = \int_0^{s_\phi} E_\phi(\sigma)\sigma^{-2}d\sigma. \quad (3)$$

It is convenient to rewrite $E_\phi \equiv (\chi\eta^3/\nu)\tilde{E}_\phi$, where $\tilde{E}_\phi$ is nondimensional, χ is the scalar dissipation rate, and $\eta \equiv (\nu^3/\epsilon)^{1/4}$. For the dissipation of turbulent kinetic energy ϵ, Taylor's scaling is used: $\epsilon = c_\epsilon U_R^3/R$ (where U_R is the velocity of the largest eddy, R the hydraulic radius, and $c_\epsilon = 5/4$) [21,22]. Furthermore, $U_R = c_u U_b$. Thus, $\epsilon = c_\epsilon c_u^3 U_b^3/R$. Using dimensional analysis [23,24,36], a thermal analog of Taylor's scaling can be formulated as $\chi = c_\chi \Delta T_R^2 U_R/R/\mathrm{Pr}$, where c_χ is a constant, ΔT_R is the temperature difference across the largest eddy. The difference between the wall- and bulk temperatures is $\Delta T = c_T \Delta T_R$. Then, $\chi = c_\chi c_u c_T^2 \mathrm{Pr}^{-1}\Delta T^2 U_b/R$. Applying the latter to Eq. (3), while using $x = \sigma/R$ yields

$$t_s^2 = \frac{c_\chi c_T^2}{c_\epsilon^{3/4} c_u^{5/4}}\left(\frac{U_b R}{\nu}\right)^{-5/4}\frac{\Delta T^2}{\mathrm{Pr}}\int_0^{s_\phi/R}\tilde{E}_\phi(x)x^{-2}dx. \quad (4)$$

The most important characteristics of the scalar spectrum E_ϕ (see Fig. 2) are $E_\phi \sim \sigma^{5/3}$, which is valid for the inertial convective range, $E_\phi \sim \sigma^{17/3}$ for the inertial diffusive range (when $\mathrm{Pr} < 1$), and $E_\phi \sim \sigma$ for the viscous-convective range (when $\mathrm{Pr} > 1$) [25]. Hill [26] derived several physical models for the scalar spectrum that can reproduce this rich structure. The simplest of these models is written as

$$\tilde{E}_\phi(x) = \beta Q^{5/2}F(x), \quad (5)$$

where

$$F(x) \equiv \left(y(x)^{-5/3} + y(x)^{-1}\right)$$
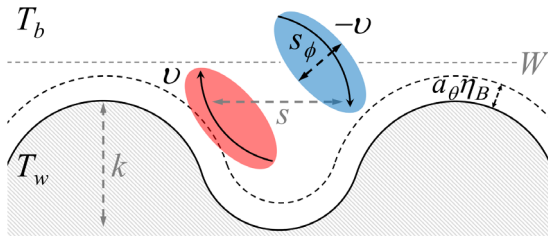$$\times \exp\left\{-A\left(\frac{3}{2}y(x)^{4/3} + y(x)^2\right)\right\}, \quad (6)$$

FIG. 1. Sketch of a rough wall at a temperature T_w and with elements of size k. The wall is covered by a conductive sublayer with a width of $a_\Theta\eta_B$. The bulk temperature of the flow $T_b < T_w$.
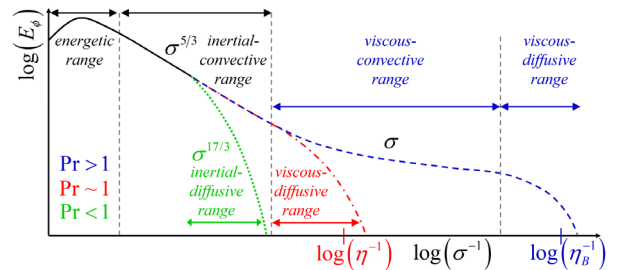

FIG. 2. Spectrum of scalar variance for fluids with different Prandtl numbers versus wave number σ^{-1}.

σ^{-1}, $A \equiv \beta \mathrm{Pr}^{-1} Q^{-2}$ and β is the Obukhov-Corrsin constant [27,28]. Q is a free parameter that was determined by comparing Eq. (5) with experiments. Hill [26] determined $\beta \approx 0.68 - 0.77$ and $Q = 2.2 - 2.5$. In the last five decades or so, a wider range of values for β was found [29,30]. Because Eq. (6) does not include the energetic range, the formulation by Gioia and Chakraborty [19] is adopted by multiplying $F(x)$ by $c_e(x)$.

As the wall is covered by a conductive sublayer of size $a_\Theta \eta_B$, the largest thermal structure that fits between two roughness elements is $s_\phi/R = 2k_s/D + a_\Theta \eta_B/R$. Here, $\eta_B = \eta/\sqrt{\mathrm{Pr}}$ is the Bachelor length scale, while a_Θ is a proportionality constant. Then, as $q \sim \rho c_p \upsilon t_s$, an appropriate scaling for υ must be found [36]. Since the scaling $\upsilon = u_s$ yields results that contradict Stanton number scalings found earlier in literature, the scaling $\upsilon \sim c_\upsilon U_b$ is used instead, which leads to

$$\mathrm{St} = K_T \left[\mathrm{Pr}^{-1} \mathrm{Re}^{-5/4} \int_0^{s_\phi/R} c_e(x) F(x) x^{-2} dx \right]^{1/2}, \quad (7)$$

where $K_T = c_\upsilon \sqrt{\beta Q^{5/2} (c_\chi c_T^2 / c_\epsilon^{3/4} c_u^{5/4})(\frac{1}{2})^{-5/4}}$.

Equation (7), is compared to a database consisting of both experimental and numerical data: (1) Dipprey and Sabersky [11] (experimental; close packed granular surface); (2) MacDonald *et al.* [16] (numerical, sinusoidal roughness), and (3) Peeters and Sandham [17] (numerical; grit-blasted surface). The aforementioned numerical studies are direct numerical simulations (DNS), in which all scales of motion and scalar transfer are resolved. The database was extended by performing additional DNS of channel flows past a grit-blasted surface with nonunity Prandtl numbers (Pr $= 2 - 6$). Between these sources of data, a large range of relevant parameters is covered: $\mathrm{St} = 1.2 \times 10^{-3} - 7.7 \times 10^{-3}$, $\mathrm{Re} = 6.8 \times 10^3 - 4.9 \times 10^5$, Pr $= 0.7 - 6.0$ and $k_s/D = 0.0024 - 0.11$.

The integral in Eq. (7) is evaluated by setting $Q = 2.5$, $\beta_2 = 0.7$, $\gamma = 6.783$, and $a_\Theta = 3.3$. Furthermore, K_T is determined such that the Reynolds analogy, $\mathrm{St} = C_f/2$, (valid for smooth wall conditions and when Pr $= 1$) is obeyed, which results in $K_T = 0.087$. To investigate if Eq. (7) can predict the correct trend of $\Delta\Theta^+$, a value for k_s is chosen first. By subsequently choosing a range of Re_τ, a corresponding range of k_s^+ is obtained. Then for every Re_τ value, corresponding bulk Reynolds numbers for both rough and smooth walls, i.e., $\mathrm{Re}_{b,r}$, $\mathrm{Re}_{b,s}$ are computed using the recursive relation $\mathrm{Re}_b = 2\mathrm{Re}_\tau/\sqrt{C_f(\mathrm{Re}_b, k_s)/2}$. Thereafter, $C_{f,r}$, $C_{f,0}$, $\mathrm{St}_{f,r}$, and $\mathrm{St}_{f,0}$ and thus $\Delta\Theta^+$ can be computed. In Fig. 3, predictions of $\Delta\Theta^+$ are compared with results obtained from two different DNS databases. It is clear that Eq. (7) yields excellent agreement for smaller values of k_s^+. However, the same relation does not predict that $\Delta\Theta^+$ levels off for large k_s^+.
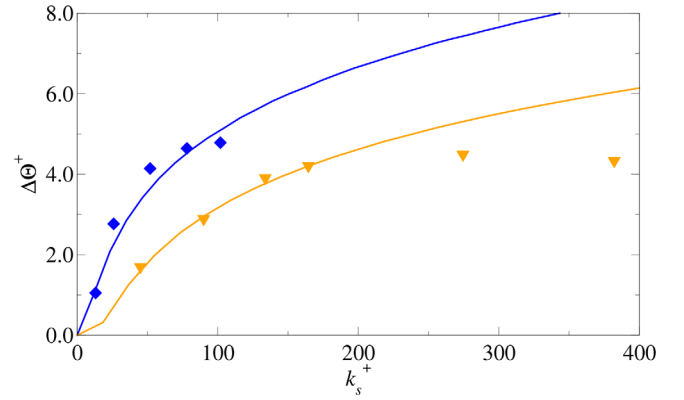

FIG. 3. $\Delta\Theta^+$ vs the sand grain equivalent wall roughness height as predicted by Eq. (1) while using Eq. (7) to compute St_r and St_s (solid blue and solid yellow lines). DNS by MacDonald *et al.* [16], Pr $= 0.7$ (yellow inverted triangles), DNS by Peeters and Sandham [17], Pr $= 1.0$ (blue diamonds).

To investigate further, the role of the different scales of scalar turbulence—the energetic, inertial-convective, and viscous- convective and dissipative range of the scalar spectrum—are analyzed. The effect of the energetic range can be omitted by setting $c_e(x) = 1$. Looking at Fig. 4, two conclusions can be drawn. First, the energetic range is not the cause of the plateau in the scalar wall roughness function. Second, the energetic range must affect heat transfer in the presence of a rough wall adversely, as the magnitude of $\Delta\Theta^+$ is larger for all k_s^+ when the energetic range is omitted. This result also shows that the effect of the inertial and dissipative range must outweigh the effect of the energetic range.

To isolate the role of the inertial-convective (IC) range, the following limit can be considered. When $y \ll 1$, Eq. (6) reduces to

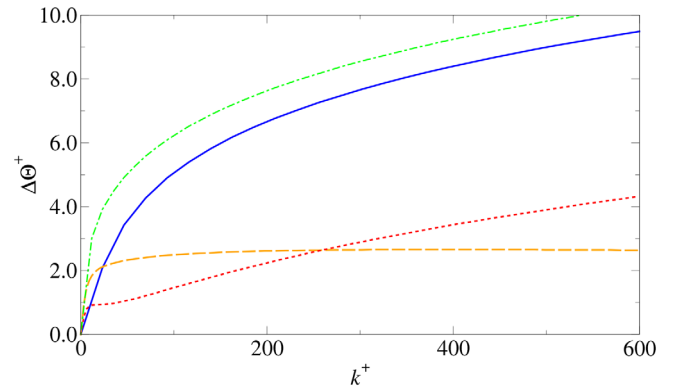$$F^{IC}(x) = y(x)^{-5/3}. \quad (8)$$

FIG. 4. $\Delta\Theta^+$ while considering the full scalar spectrum (5) (solid blue line), no energy containing range (green dash-dotted line), the inertial-convective range (8) (red dotted line) and the viscous- convective and diffusive range (10) (yellow dashed line). In this example, Pr $= 1$.

If $F^{IC}(x)$ is now substituted for $F(x)$ in Eq. (6), Eq. (7) reduces to

$$\mathrm{St} = K'_T \frac{\left(2\frac{k_s}{D}\mathrm{Re}^{3/4}\mathrm{Pr}^{1/2} + a_\Theta b'\right)^{1/3}}{\mathrm{Re}^{1/4}\mathrm{Pr}^{2/3}}, \qquad (9)$$

where $K'_T \equiv K_T\sqrt{3/2}/(b'^{5/6}Q^{5/4})$. When only the inertial-convective range is considered—shown in Fig. 4 as well—$\Delta\Theta$ appears to almost level off, only to increase thereafter. Therefore, $\Delta\Theta^+$ leveling off is not the result of the inertial-convective range either.

The previous result leaves the viscous- convective and diffusive range. In the limit $A \ll 1$ and $y \gg 1$, while neglecting the energy containing scales, Eq. (6) reduces to the viscous- convective and diffusive form predicted by Batchelor [31],

$$F^{VC}(x) = y(x)^{-1} \exp\left\{-Ay(x)^2\right\}. \qquad (10)$$

Please note that $A = 0.112$, when $\mathrm{Pr} = 1$. Replacing F with F^{VC} results in

$$\mathrm{St} = \frac{K''_T}{\mathrm{Pr}^{1/2}\mathrm{Re}^{1/4}}\sqrt{E_1\left\{\frac{C_1}{(2\frac{k_s}{D}\mathrm{Re}^{3/4}\mathrm{Pr}^{1/2} + C_2)^2}\right\}}, \quad (11)$$

where E_1 is the exponential integral, $E_1(x) \equiv \int_1^\infty x^{-1}\exp(-x)dx$ [32], $C_1 \equiv b'^2 Q\beta_2$ and $C_2 \equiv a_\Theta b'$ and $K''_T \equiv K_T/\sqrt{2b'Q^{3/2}}$. For a more convenient form, $E_1(x) \approx -\gamma - \ln(x)$ for sufficiently small x (where $\gamma = 0.577\cdots$ is the Euler-Mascheroni constant). Looking again at Fig. 4 shows that the wall roughness function levels off at large values of k_s^+ when only the viscous- convective and diffusive range is considered. Therefore, the fact that $\Delta\Theta^+$ levels off must be the result of the interaction between the viscous- convective and diffusive scales and the rough wall.

It is interesting to note that the inertial-convective range produces a different Prandtl number scaling than the viscous-convective range does. Equation (9) has two important limits. As $k_s \to 0$, then $\mathrm{St} \sim C_f\mathrm{Pr}^{-2/3}$, which is consistent with both the Chilton-Colburn analogy and the Gnielinski correlation for smooth walls [33]. However, when $k_s/D \gg \frac{1}{2}a_\Theta b'\mathrm{Re}^{-3/4}\mathrm{Pr}^{-1/2}$, it becomes clear that $\mathrm{St} \sim \mathrm{Pr}^{-1/2}$. Furthermore, Strictler's scaling appears: $\mathrm{St} \sim (k_s/D)^{1/3}$, which suggests that an analogy between skin friction and heat transfer may exist when heat transfer by the inertial scales is dominant. Following Gioia and Chakraborty [19], it can be shown that $C_f \sim K\sqrt{3/2}\times (2k_s/D)^{1/3}$ when $2k_s/D \gg ab'\mathrm{Re}^{-3/4}$. Likewise, when $2k_s/D \gg a_\Theta b'\mathrm{Re}^{-3/4}\mathrm{Pr}^{-1/2}$, $\mathrm{St} \sim 2^{1/3}K'_T\mathrm{Pr}^{-1/2}(k_s/D)^{1/3}$. Thus,

$$\mathrm{St} \sim \left(\frac{K'_T}{K\sqrt{3/2}}\right)C_f(k_s/D)\mathrm{Pr}^{-1/2}. \qquad (12)$$
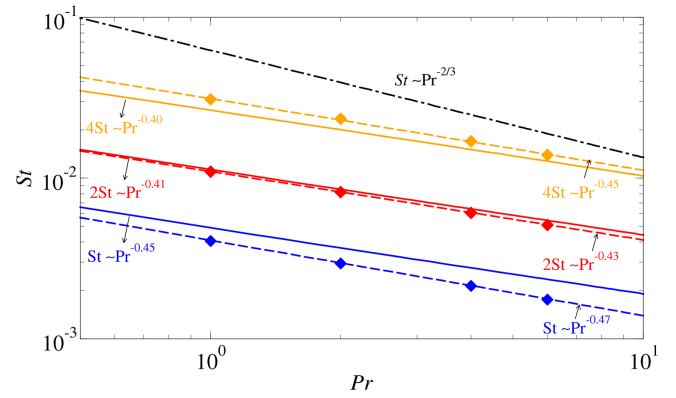

FIG. 5. Stanton number as a function of the Prandtl number. DNS data: $k_s/D = 0.0181$ (blue diamonds), $k_s/D = 0.0363$ (red diamonds), $k_s/D = 0.0725$ (yellow diamonds) with corresponding power law fit (dashed lines; scaling shown on the right). Predictions by Eq. (11) (solid lines, scaling shown on the left). The scaling $\mathrm{Pr}^{-2/3}$ (dash-dotted line) is shown as well.

This analogy can only be true when the characteristic size of the wall roughness is much larger than both the Kolmogorov- and Batchelor scale, and when the contribution of the inertial convective scales is dominant. The latter occurs when $\mathrm{Re} \sim 10^8$ [19]. Thus, it is logical that this analogy is not valid in the experimental and numerical studies of heated ducts, as those studies were performed at much lower Reynolds numbers. However, the scaling $\mathrm{St} \sim \mathrm{Pr}^{-1/2}$ does appear in meteorological studies where Reynolds numbers are typically much larger than flows encountered in laboratories or industry [34].

Compared to Eq. (9), the Prandtl number scaling in Eq. (11) is not readily apparent. Therefore, Eq. (11) is compared to the results of the DNS database in Fig. 5. Two separate observations can be made. First, the DNS results scale as Pr^{-n}, where $n = 0.43 - 0.47$. Second, Eq. (11) reproduces a similar scaling with $n = 0.41 - 0.45$. Consequently, it can be concluded that the scaling $\mathrm{St} \sim \mathrm{Pr}^{-0.44}$ found by Dipprey and Sabersky [11] experimentally must stem from the contribution of the viscous- convective and diffusive range.

The previous analyses regarding the trend of the wall roughness function and the Prandtl number scaling suggest that heat transfer in the presence of a rough wall can be understood by considering the viscous- convective and diffusive range only—at least for sufficiently small Reynolds numbers, i.e., $\mathrm{Re} \ll 10^8$. To test this hypothesis, Eq. (11) is fitted to both the numerical and experimental database. C_1 is determined by the properties of the scalar spectrum, while K''_T and C_2 are considered fittable parameters. K''_T and C_2 may depend on the characteristics of the surface; a similar argument was made by Goldenfeld [35] who stated that different types of roughness may alter the scaling of the friction factor. Fitting Eq. (11) against the DNS database ($\mathrm{Pr} = 1 - 6$) by minimizing the least-squares error yields $K''_T = 3.01 \times 10^{-2}$, and $C_2 = 15.4$.
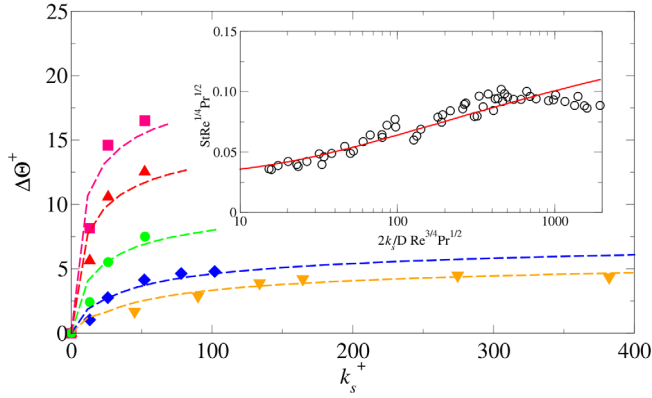
FIG. 6. $\Delta\Theta$ vs k_s^+ as predicted by using (11) (dashed lines). DNS by MacDonald *et al.* [16], Pr = 0.7 (yellow inverted triangles); DNS by Peeters and Sandham [17], Pr = 1 (blue diamonds), DNS current study, Pr = 2 (green solid circles), Pr = 4 (red triangles), Pr = 6 (red solid squares). Inset: experimental data by Dipprey and Sabersky [11] (open circles), prediction by Eq. (11) (red solid line).

In Fig. 6 it is shown that Eq. (11) is able to reproduce the trend of the scalar wall roughness function $\Delta\Theta^+$ very well. However, a plateau is not predicted. Another interesting feature of Eq. (11) is that the Stanton number data should collapse onto a single curve if $\mathrm{StRe}^{1/4}\mathrm{Pr}^{1/2}$ is plotted against $2(k_s/D)\mathrm{Re}^{3/4}\mathrm{Pr}^{1/2}$. This prediction is shown in the inset of Fig. 6, along with the experimental data of Dipprey and Sabersky [11]. Equation (11) (with $C_1 = 3.9 \times 10^{-2}$, $C_2 = 50.8$) describes the experimental data accurately up to $2(k_s/D)\mathrm{Re}^{3/4}\mathrm{Pr}^{1/2} \approx 700$. Beyond this value, the experimental data show a downward trend that is not predicted by the current theory. These results mean that the turbulent heat transfer in the presence of a rough wall is well described by the motions in the viscous- convective and diffusive range for relatively small values of k_s/D. Noting that $\eta_B/D = 1/2b'\mathrm{Re}^{-3/4}\mathrm{Pr}^{-1/2}$, this statement can be rephrased in physical terms as; turbulent heat transfer in the presence of a rough wall is dominated by the eddies of the viscous-convective and diffusive range, when the roughness size k_s is smaller than 36 times the Batchelor length scale η_B.

[1] L. F. Richardson, Atmospheric diffusion shown on a distance-neighbour graph, Proc. R. Soc. A **110**, 709 (1926).

[2] L. D. Landau and E. M. Lifshitz, *Fluid Mechanics* (Pergamon Press, Oxford, 1987).

[3] J. Jiménez, Turbulent flows over rough walls, Annu. Rev. Fluid Mech. **36**, 173 (2004).

[4] D. Chung, N. Hutchins, M. P. Schultz, and K. A. Flack, Predicting the drag of rough surfaces, Annu. Rev. Fluid Mech. **53**, 439 (2021).

[5] A. N. Kolmogorov, The local structure of turbulence in incompressible viscous fluid for very large Reynolds numbers, Proc. R. Soc. A **434**, 9 (1991).

[6] U. Frisch, *Turbulence: The Legacy of A. N. Kolmogorov* (Cambridge University Press, Cambridge, England, 1995).

[7] L. Prandtl, *Essentials of Fluid Dynamics* (Blackie & Son, London, 1953).

[8] F. H. Clauser, Turbulent boundary layers in adverse pressure gradients, J. Aeronaut. Sci. **21**, 91 (1954).

[9] F. R. Hama, Boundary-layer characteristics for smooth and rough surfaces, Trans. Soc. Nav. Archit. Mar. Eng. **62**, 333 (1954).

[10] M. P. Schultz and K. A. Flack, Turbulent boundary layers on a systematically rough wall, Phys. Fluids **21**, 015104 (2009).

[11] D. F. Dipprey and R. H. Sabersky, Heat and momentum transfer in smooth and rough tubes at various Prandtl numbers, Int. J. Heat Mass Transfer **6**, 329 (1963).

[12] P. R. Owen and W. R. Thomson, Heat transfer across rough surfaces, J. Fluid Mech. **15**, 321 (1963).

[13] P. Forooghi, M. Stripf, and B. Frohnapfel, A systematic study of turbulent heat transfer over rough walls, Int. J. Heat Mass Transfer **127**, 1157 (2018).

[14] J. Bons, A critical assessment of Reynolds analogy for turbine flows, Trans. Am. Soc. Mech. Eng. **127**, 160 (2005).

[15] A. M. Yaglom, Similarity laws for constant-pressure and pressure-gradient turbulent wall flows, Annu. Rev. Fluid Mech. **11**, 505 (1979).

[16] M. MacDonald, N. Hutchins, and D. Chung, Roughness effects in turbulent forced convection, J. Fluid Mech. **861**, 138 (2019).

[17] J. W. R. Peeters and N. Sandham, Turbulent heat transfer in channels with irregular roughness, Int. J. Heat Mass Transfer **138**, 454 (2019).

[18] J. W. R. Peeters, Modelling turbulent heat transfer in rough channels using phenomenlogical theory, J. Phys. Conf. Ser. **2116**, 012025 (2021).

[19] G. Gioia and P. Chakraborty, Turbulent Friction in Rough Pipes and the Energy Spectrum of the Phenomenological Theory, Phys. Rev. Lett. **96**, 044502 (2006).

[20] J. Nikuradse, Strömingsgesetze in rauhen Rohren, Beilage zu Forshung auf dem gebiet des Ingeniurswesens, Forshungsheft 361 (1933), Ausgabe B, Band 4.

[21] G. I. Taylor, Statistical theory of turbulence, Proc. R. Soc. A **151**, 421 (1935).

[22] D. Lohse, Crossover from High to Low Reynolds Number Turbulence, Phys. Rev. Lett. **73**, 3223 (1994).

[23] C. Béguier, I. Dekeyser, and B. E. Launder, Ratio of scalar and velocity dissipation time scales in shear flow turbulence, Phys. Fluids **21**, 307 (1978).

[24] H. Kawamura, K. Ohsaka, H. Abe, and K. Yamamoto, DNS of turbulent heat transfer in channel flow with low to medium-high Prandtl number fluid, Int. J. Heat Fluid Flow **19**, 482 (1998).

[25] K. R. Sreenivasan, Turbulent mixing: A perspective, Proc. Natl. Acad. Sci. U.S.A. **116**, 18175 (2019).

[26] R. J. Hill, Models of the scalar spectrum for turbulent advection, J. Fluid Mech. **88,** 541 (1978).

[27] A. M. Obukhov, Structure of the temperature field in turbulent flow, Izv. Akad. Nauk. SSSR, Ser. Geogr. i Geofiz. **13,** 58 (1949).

[28] S. Corrsin, On the spectrum of isotropic temperature fluctuations in isotropic turbulence, J. Appl. Phys. **22,** 469 (1951).

[29] K. R. Sreenivasan, The passive scalar spectrum and the Obukhov-Corrsin constant, Phys. Fluids **8,** 189 (1996).

[30] K. P. Shete, D. J. Boucher, J. J. Roley, and S. M. de Bruyn Kops, Effect of viscous-convective subrange on passive scalar statistics at high Reynolds number, Phys. Rev. Fluids **7,** 024601 (2022).

[31] G. K. Batchelor, Small-scale variation of convected quantities like temperature in turbulent fluid. 1. General discussion and the case of small conductivity, J. Fluid Mech. **5,** 113 (1959).

[32] M. Abramowitz and I. A. Stegun, *Handbook of Mathematical Functions with Formulas, Graphs, and Mathematical Tables*, 9th Dover printing, 10th GPO Printing ed. (Dover, New York, 1964).

[33] V. Gnielinski, Neue gleichungen für den wärme- und den stoffübergang in turbulent durchströmten rohren und kanälen, Forsch. Ingenieurwes. A **41,** 8 (1975).

[34] Q. Li, E. Bou-Zeid, S. Grimmond, S. Zilitinkevich, and G. Katul, Revisiting the relation between momentum and scalar roughness lengths of urban surfaces, Q. J. R. Meteorol. Soc. **146,** 3144 (2020).

[35] N. Goldenfeld, Roughness-Induced Critical Phenomena in a Turbulent Flow, Phys. Rev. Lett. **96,** 044503 (2006).

[36] See Supplemental Material at http://link.aps.org/supplemental/10.1103/PhysRevLett.131.134001 for the equations appearing in this work are derived here in a step-by-step manner. Furthermore, the thermal analog of Taylor's scaling and the velocity scaling used in the Stanton relation are discussed.